Published in final edited form as:
Stem Cells. 2012 October ; 30(10): 2065–2075. doi:10.1002/stem.1139.

Phosphosulindac (OXT-328) selectively targets breast cancer stem cells *in vitro* and in human breast cancer xenografts

Caihua Zhu[1], **Ka-Wing Cheng**[1], **Nengtai Ouyang**[1], **Liqun Huang**[1], **Yu Sun**[1], **Panayiotis P. Constantinides**[2], and **Basil Rigas**[1,*]

[1]Division of Cancer Prevention, Department of Medicine, Stony Brook University, Stony Brook, New York

[2]Medicon Pharmaceuticals, Inc., Stony Brook, New York

Abstract

Pharmacological targeting of breast cancer stem cells (CSCs) is highly promising for the treatment of breast cancer, as the small population of CSCs appears responsible for tumor initiation and progression and also for resistance to conventional treatment. Here we report that the novel phosphosulindac (OXT-328, PS) selectively and effectively eliminates breast CSCs both *in vitro* and *in vivo*. PS reduced cell proliferaition and induced apoptosis in various breast CSCs. Breast CSCs are resistant to conventional cancer drugs but are sensitive to PS. Long-term treatment with PS of mixtures of cultured breast CSCs with breast cancer cells preferentially eliminated the CSCs. PS impaired the ability of CSCs to form mammospheres and markedly suppressed the expression of CSC-related genes. More importantly, PS prevented by half ($p=0.06$) the formation of tumors initiated by CSCs in immunodeficient mice, and inhibited by 83% ($p<0.05$) the growth of already formed breast cancer xenografts, reducing the proportion of CSCs in them. PS suppressed the Wnt/β-catenin pathway by stimulating the degradation of β-catenin and its relocalization to the cell membrane; and also blocked the epithelial-mesenchymal transition (EMT) and the generation of breast CSCs. These results indicate that PS has a strong inhibitory effect against breast cancer, acting, at least in part, by targeting CSCs through a signaling mechanism involving Wnt signaling.

Keywords

CSCs; phosphosulindac; Wnt/β-catenin; EMT; breast cancer

Introduction

Despite advances in our understanding of breast cancer biology, the development of effective strategies for its prevention and treatment represents great challenges. The main reason for our failure to control breast cancer is thought to be our inability to eliminate

*To whom correspondence should be addressed. Division of Cancer Prevention, HSC, T-17 Room 080, Stony Brook, NY 11794-8173, Tel: +1 631-444-9538; Fax: +1 631-444-9553; basil.rigas@stonybrook.edu.

Author contributions: C.Z.: collection and/or assembly of data, data analysis and interpretation, manuscript writing, and final approval of manuscript; K.C., N.O., L.H., and Y.S.: design, collection and/or assembly of data, data analysis and interpretation, manuscript writing, and final approval of manuscript; P.C.: provision of study material, and final approval of manuscript; B.R.: conception and design, financial support, provision of study material, data analysis and interpretation, manuscript writing, and final approval of manuscript.

Disclosure of potential conflicts of interest: B.R. has an equity position in Medicon Pharmaceuticals, Inc. and P.C.C. is affiliated with the same.

tumor initiating cells, also known as cancer stem cells (CSCs). CSCs may originate from stem cells, progenitor cells, or other differentiated cancer cells [1, 2]. Although comprising only a small fraction of all cells in tumors, CSCs are solely responsible for generating the bulk of the tumor through continuous self-renewal and differentiation. Several markers identify breast CSCs, including enhanced acetaldehyde dehydrogenase (ALDH) expression/activity and the $EpCAM^{+}CD44^{+}CD24^{-}$ phenotype [3–5].

There is an intimate link between epithelial-mesenchymal transition (EMT) and the acquisition of stem cell properties [6–8]. The evidence for this link includes a) the demonstration that induction of EMT in a human mammary epithelial cell line (HMLE) transformed its baseline phenotype ($CD44^{low}/CD24^{high}$) into one with a breast stem cell-like phenotype ($CD44^{high}/CD24^{low}$) with increased ability to form mammospheres; b) stem-like cells from either normal or malignant breast tissue express EMT markers, such as high levels of vimentin, Snail, Slug and Twist and low levels of E-cadherin; and c) *Ras*-transformed HMLEs (HMLERs) form mammospheres and initiate tumors more efficiently after they are induced into EMT [6]. These and other studies [5, 9] provide strong evidence that EMT could generate cancer cells with stem cell properties. A corollary to this is that key signaling pathways in EMT, like TGFβ and Wnt/β-catenin, are potentially useful drug targets for CSCs elimination.

Unlike most cells within a tumor, CSCs are particularly resistant to conventional chemotherapy [10, 11]. This property not only explains the limitations of current chemotherapeutic agents, but also suggests that compounds suppressing CSCs should overcome drug resistance and reduce tumor relapses. Therefore, agents that targeting signaling pathways crucial to the self-renewal of CSCs, such as Wnt/β-catenin, Notch and Hedgehog can be particularly effective. [12]. Of interest, the Wnt/β-catenin signaling pathway, in addition to EMT and the self-renewal of CSCs, plays a role in a third process, the growth of bulk cell tumor populations [13]. Thus, the ubiquitous role of Wnt/β-catenin signaling in different types of cancer cells implies that targeting it could produce a robust antitumor effect.

Sulindac, a non-steroidal anti-inflammatory drug (NSAID), is in wide clinical use. Animal and clinical studies have shown that, like other NSAIDs, sulindac is effective in the prevention of cancer, including cancers of the colon and breast [14]. Sulindac's inhibition of tumorigenesis is partly attributed to its inhibition of COX-2, Wnt/β-catenin and NF-κB signaling [15–19]. However, its cancer preventive effect is relatively weak and long-term administration of sulindac is associated with significant side effects [20, 21]. The novel compound phosphosulindac (PS, OXT-328), a derivative of sulindac, is more effective than conventional sulindac against colon cancer and appears to be much safer [22, 23]. Here, we show both *in vitro* and *in vivo* that PS can selectively kill breast CSCs and reduce their tumor-initiating ability. PS targets breast CSCs by inhibiting Wnt/β-catenin signaling and EMT, and this effect provides a strong rationale for the evaluation of PS for the treatment of breast cancer.

MATERIALS AND METHODS

Reagents and cell culture

Phosphosulindac (OXT-328) was a gift from Medicon Pharmaceuticals, Inc, Setauket, NY. B27, Annexin V-APC and 2',7'-dichlorodihydrofluorecein diacetate (DCFDA) were purchased from Invitrogen (Carlsbad, CA). DMEM/F12 medium was from Mediatech Inc (Manassas, VA). CD44-APC antibody was purchased from eBioscience (San Diego, CA). CD24-PE, epidermal growth factor and basic fibroblast growth factor were from BD Transduction (San Jose, CA, USA). SK-3rd cells were provided by Dr. Erwei Song (Sun-

Yat-Sen University, China) and cultured in ultralow attachment culture dish (Corning Inc, N.Y.) in DMEM/F12 media supplemented with B27, 20 ng/ml EGF, 20ng/ml bFGF, 5 μg/ml insulin and 0.4% bovine serum albumin. HMLER, HMLER^{shCTRL} and HMLER^{shECAD} cells were provided by Dr. RA Weinberg (MIT, Cambridge, MA) and cultured in DMEM/F12 with 10% FBS, 10 μg/ml insulin, 10 ng/ml EGF, 0.5 μg/ml hydrocortisone and 1 μg/ml puromycin.

Cell kinetic assays

Cell viability was measured by the 3-(4, 5-dimethylthiazol-2-yl)-2, 5-diphenyltetrazolium bromide (MTT) assay following the protocol of the manufacturer (Roche Diagnostics, South San Francisco, CA). To measure cell death, cells were treated with PS for 24 h, harvested by trypsinization, stained with APC-conjugated Annexin V and propidium iodide (PI) according to the manufacturer's protocol and analyzed by flow cytometry. For cell cycle analysis, cells were fixed with cold 70% ethanol and stained with PI and subjected to flow cytometric analysis following standard protocols.

Western blotting

Following treatment, cells were lysed on ice with RIPA buffer for 30 min. For each sample, 20 μg of cell lysate were loaded onto SDS-electrophoresis gel and transferred onto a nitrocellulose membrane. The membrane was then immunoblotted with primary antibodies followed by secondary antibodies conjugated with horseradish peroxidase (HRP) from Santa Cruz Biotechnology. Enhanced chemiluminescence (ECL) was used to visualize the bands on X-ray film.

Immunohistochemistry and immunofluorescence

Breast cancer xenografts were fixed in formalin, embedded in paraffin block and cut into 5 μm thick sections. Tissue sections were deparaffinized with xylene and rehydrated using decreasing concentrations of alcohol. After antibody retrieval, sections were blocked with serum for 2 h, and then incubated with a 1:100 dilution of primary antibodies at 4 °C overnight. After three washes with PBST (PBS + 0.05% Tween 20) for 15 min, tissue sections were incubated for 2 h with fluorophore-conjugated secondary antibodies diluted 1:400 and covered with mounting medium with 4'-6-diamidino-2-phenylindole (DAPI) (Santa Cruz Biotechnology) or PI. The slides were examined and photographed using a Nikon microscope (Nikon Eclipse TE-2000-S) with a Wide Zoom Camera.

Real-time quantitative reverse transcription-PCR

For gene expression assays, total RNA was extracted from cells using the Trizol reagent (Sigma) and cDNA was obtained using Moloney murine leukemia virus reverse transcriptase and RNase H minus (Sigma). Typically, 200 ng of template total RNA and 100 ng of random hexamers were used per reaction. Real-time PCR amplification was performed using SYBR master mix and specific PCR primers in an MJ Opticon instrument (Bio-Rad). Relative quantification of each target was normalized to an endogenous control (β-actin) using a comparative C_t method.

Mammosphere formation

Mammospheres were cultured in ultralow attachment 96-well plates in serum-free DMEM/F12 media, supplemented with B27, 0.4% bovine serum albumin, 20 ng/mL EGF, 20 ng/mL bFGF, 5 μg/mL insulin and 0.75% methylcellulose.

Animal studies

For *cancer prevention* studies, six-week-old female BALB/c nude mice (Charles River, Troy, NY; n=7/group) were treated by gavage with PS 100 mg/kg/d or vehicle (corn oil). Five days later, mice were inoculated subcutaneously with 2×10^3 SK-3rd cells on each flank. Treatment with PS 100 mg/kg/d or vehicle 5 d/wk continued until sacrifice. For *cancer treatment* studies, 6-wk-old female Hsd:NIHS-*Lyst*^{bg}*Foxn1*^{nu}*Btk*^{xid} mice (Harlan Laboratories; n=10/group) were inoculated with 5×10^4 HMLER$^{TGF\beta1}$ cells into the most cephalad mammary fat pad per mouse. When palpable tumors developed, mice were randomly divided into 2 groups and treated with vehicle (corn oil) or PS 150 mg/kg/d 5 d/wk. Treatment continued for 6 weeks. Tumor size was determined with a digital microcaliper, and tumor volume was calculated using the formula: volume = [length × width × (length × width/2) ×0.56]. Tumor growth inhibition was calculated by dividing the percent increase from baseline of the tumor volume of the treated group over the corresponding percent volume increase of the control group. All animal studies were approved by the Institutional Animal Care and Use Committee of Stony Brook University and performed in accordance with relative policies and protocols.

Results

PS effectively and selectively inhibits the growth of human breast CSCs

To evaluate the effect of PS on breast cancer and breast CSCs, we used several genetically and phenotypically different cell lines (Table S1): HMLER/HMLER$^{TGF\beta1}$, HMLER^{shCTRL}/HMLER^{shECAD}, SKBR3/SK-3rd, and MDA-MB-231. HMLER is a *Ras*-transformed HMLE, which has been immortalized by overexpressing the human catalytic subunit of telomerase and SV40 large T and small t antigens [24]. HMLER$^{TGF\beta1}$ are HMLER cells induced into EMT by TGF β1 treatment. HMLER^{shCTRL} are HMLER cells transfected with the control vector, while HMLER^{shECAD} cells were established by knocking down the human *CDH1* gene (encodes E-cadherin) in experimentally transformed HMLER breast cancer cells [7]. *CDH1* silencing triggered EMT and cells with the mesenchymal phenotype gained stem cell properties [6]. SK-3rd cells, enriched by consecutively passaging SKBR3 breast cancer cells in NOD/SCID mice treated with epirubicin, display the CSC properties of self-renewal, multipotent differentiation and a high rate of tumor initiation [25]. HMLER$^{TGF\beta1}$, HMLER^{shECAD} and SK-3rd are enriched CD44^{high}/CD24^{low} cells, while their parental cells lines are CD44^{low}/CD24^{high} (Fig. S1). In our studies, 2,000 SK-3rd cells, 10,000 HMLER$^{TGF\beta1}$ and 10,000 HMLER^{shECAD} cells could efficiently initiate tumors in NOD/SCID mice (data not shown). MDA-MB-231 cells are derived from triple negative human breast adenocarcinoma with an aggressive mesenchymal phenotype.

PS 50 μM induced cycle arrest in HMLER^{shECAD} cells after 24 h of treatment (48.3% of treated cells in G_0/G_1 phase, compared with 38.4% in controls; Fig. 1A). PS induced cell death in HMLER^{shECAD} cells at a higher concentration (180 μM) with 15.5% dead cells at 24 h vs. 6.7% in controls (Fig. 1B). Similar results were obtained in SK-3rd cells. The proportion of cells in G_0/G_1 phase increased from 24.5% to 55.4%, and the proportion of dead cells increased from 3.8% to 91.5% (same concentrations of PS).

It is challenging to eradicate CSCs because of their innate resistance to cancer drugs [26]. We compared the drug sensitivity of these two CSC lines (HMLER^{shECAD} and SK-3rd) to that of their parental cell lines (HMLER^{shCTRL} and SKBR3). As shown in Fig. 1C, both CSC lines were much less sensitive to conventional cancer drugs, with their 48-h IC_{50}s being 5–20 fold higher than those of their parental cell lines (Table 1). However, PS inhibited the growth of CSCs as effectively as that of their parental cells. These results

demonstrated that, in contrast to conventional chemotherapeutic agents, breast CSCs are sensitive to PS.

We then tested the effect of long-term treatment with PS on breast CSCs. Since the percentage of $CD44^{high}/CD24^{low}$ cells in HMLER cells is very low (<5%), it is difficult to compare the sensitivity of CSCs and non-CSCs by determining the proportion of $CD44^{high}/CD24^{low}$ cells in total HMLERs after treatment with PS. Thus, we mixed $HMLER^{shECAD}$ cells with $HMLER^{shCTRL}$ cells at a ratio of 1:1. These mixed cell populations were treated with 30 μM PS for 7 days. Few dead cells were observed during treatment, and all living cells were stained with antibodies against CD24 and CD44 and analyzed by flow cytometry. PS reduced the proportion of $HMLER^{shECAD}$ cells in the entire population 3 fold (from 34.5 % to 12.0%, Fig. S2A). We then assessed the selectivity of the effect of PS on CSCs that exist naturally as a subpopulation within HMLER cells rather than in those experimentally induced into EMT. To this end, we isolated by fluorescence-activated cell sorting $CD44^{high}/CD24^{low}$ and $CD44^{low}/CD24^{high}$ HMLER cells and mixed them in a ratio of 1:1. After treating this cell population with PS for 7 days, the proportion of $CD44^{high}/CD24^{low}$ cells was 9.7%, compared to 43.1% in the untreated control; for comparison, the parental compound sulindac exerted a quite weak effect on eliminating $CD44^{high}/CD24^{low}$ cells (35.4%) (Fig. 1D). Conventional cancer drug taxol, in contrast, markedly enriched the proportion of these cells (77.2%) after 7 day treatment. We then determined the proliferative state of $HMLER^{shCTRL}$ and $HMLER^{shECAD}$ cells after treatment with PS for 7 days. . While 15 μM and 30 μM PS caused 26.4% and 39.4% reduction of BrdU-positive cells respectively in $HMLER^{shEcad}$ cells, they showed minimal effects on $HMLER^{shCTRL}$ cells (3.9% and 5.6% reduction respectively, Fig. S2B). These data showed that PS exerted a more potent effect on proliferation inhibition in $HMLER^{shECAD}$ cells than in $HMLER^{shCTRL}$ cells.

PS impairs mammosphere formation of breast CSCs and reduces stem cell-related gene expression

Breast CSCs are able to form non-adherent spherical clusters of cells, termed mammospheres and considered to result from the self-renewal properties of CSCs [27]. To evaluate whether PS could suppress the formation of mammospheres, we exposed $HMLER^{shECAD}$ cells to 30 μM PS for 2 days and then cultured them without PS for another 14 days. As shown in Fig. 2A, PS pretreatment drastically reduced the number of mammospheres formed by $HMLER^{shECAD}$ cells. To test whether this suppression was dependent on reduced proliferation caused by PS, we treated cells with or without 30 μM PS for 2 days, and then cultured them in fresh medium for another 4 days and determined their proliferation. Pretreatment with PS caused no significant growth inhibition (Fig. S2C). For SK-3^{rd} cells, as low as 5 μM PS (7% of its 48-h IC_{50}) almost completely eliminated mammospheres in 12 days (Fig. 2B). At even lower concentrations of PS, a fraction of mammospheres survived but their size was dramatically reduced (Fig. 2B, *inset*). These findings indicate the high potency of PS specifically with regards to this effect.

Since PS impaired the ability of CSCs to form mammospheres in a cytotoxicity-independent manner, we examined whether it affects the expression of transcription factors which are crucial to the stemness of CSCs. We determined the mRNA levels of a series of stem cell-related genes by real-time PCR. Salinomycin which specifically targets breast CSCs was used as a positive control [7]. As shown in Fig. 2C, salinomycin at $1\times IC_{50}$ concentration was able to reduce the expression of stem cell-related genes after 24 h of treatment (*Oct-4*, 59.7%; *BMI-1*, 24.5%; *Sox-2*, 85.1%; *Nanog*, 83.3%; *NESTIN*, 43.4%; *Notch-1*, 47.3%; and *c-Myc*, 24.2%), with the exception of TWIST, MDR-1 and ABCG2, which were up-regulated. Compared with salinomycin, PS showed a more potent effect in down-regulating these genes (inhibition rates: *Oct-4*, 91.5%; *BMI-1*, 52.0%; *Sox-2*, 97.3%; *Nanog*, 94.2%; *NESTIN*, 76.0%; *Notch-1*, 61.4%; *ABCG2*, 79.1%; and *c- Myc*, 62.7%).

PS targets the Wnt/β-catenin pathway and reduces Snail expression blocking EMT and preventing the generation of CSCs

Aberrant activation of the Wnt pathway has been observed in various human cancers, and its critical role in CSCs is being increasingly appreciated, highlighting its potential as a therapeutic target [28–31]. A recent study showed that Wnt/β-catenin signaling is responsible for inducing EMT in the HMLER cells used here and for maintaining the resulting mesenchymal and stem cell states [8]. Currently, NSAIDs are among the most promising inhibitors of Wnt/β-catenin signaling [13] and sulindac has been reported to reduce β-catenin nuclear accumulation in colorectal cancer cells [32–34].

The activity of β-catenin-dependent Wnt signaling in $HMLER^{shECAD}$ cells is 4.2 fold higher than that in $HMLER^{shCTRL}$ cells as determined by TOPFlash β-catenin/TCF-LEF reporter assay (Fig. 3A). After treatment with PS for 24 h, β-catenin/TCF-LEF activity in $HMLER^{shECAD}$ was largely reduced (Fig. 3A). As shown in Fig. 3B, the level of β-catenin was modestly reduced after PS treatment. However, the nuclear level of β-catenin was more markedly reduced after PS treatment (Fig. 3C, 75.9% and 94.4% down-regulation by 25 μM and 50 μM PS, respectively). Similar result (Fig S4A) was also observed in $HMLER^{TGF\beta1}$ (HMLER cells induced into EMT by TGFβ1, an effect confirmed by detecting reduced E-cadherin and increased vimentin expression, and enriched for $CD44^{high}/CD24^{low}$ cells (Fig. S1 and S3A)).

We then determined by immunofluorescence the cellular localization of β-catenin in HMLER and $HMLER^{TGF\beta1}$. In HMLER cells, β-catenin localized mainly in the cell membrane; but after TGFβ1- induced EMT, most of β-catenin translocated into the cytoplasm and nucleus (Fig. 3D). PS treatment led to the relocalization of β-catenin to the cell membrane and cytoplasm, in close agreement with the results obtained by immunoblotting (Fig. 3C). Similar results were also obtained with $HMLER^{shECAD}$ cells (Fig. S4B). Post-transcriptionally, the stability of β-catenin, which is central to this pathway, is regulated by the cytoplasmic degradation complex comprised of adenomatous polyposis coli (APC), axin, casein kinase 1 (CK1) and glycogen synthase kinase 3β (GSK-3β) [35]. The kinase activity of GSK-3β is required for phosphorylation and proteasomal degradation of β-catenin. PS decreased GSK-3β phosphorylation on serine 9 (Fig. 3B), indicating a higher kinase activity of GSK-3β. This finding explains the reduced β-catenin level in PS-treated cells. Consistently, the expression of targets downstream of β-catenin such as cyclin D1 and c-Myc was also reduced (Fig. 3B). We also tested these effects in MDA-MB-231 cells, which undergo autocrine Wnt signaling [36]. As shown in Fig. S4D and S4E, the results with MDA-MB-231 cells are even more pronounced, with greater β-catenin down-regulation and relocalization. Since the transient silencing of β-catenin could slightly enrich $CD44^{low}/CD44^{high}$ cells in $HMLER^{TGF\beta1}$ cells (Fig. S4C), the suppressive effects of PS on β-catenin might acontribute to blockade or reversal of EMT.

EMT, a key developmental program, is often activated during cancer invasion and metastasis [37]. Recently, it was revealed that EMT also generates cells with stem cell properties, and that cancer cells which undergo EMT initiate tumors more efficiently [6, 7]. The zinc-finger transcriptional factor Snail triggers EMT by repressing the transcription of *E-cadherin*. Overexpressing Snail in HMLE cells ($CD44^{low}/CD24^{high}$) induces a stem-cell like phenotype ($CD44^{high}/CD24^{low}$) and increases their ability to form mammospheres [6]. Treatment of HMLER cells with TGFβ1 for 24 h increased Snail protein levels (Fig. 3E) and transformed them into the $CD44^{high}/CD24^{low}$ phenotype in 3–4 weeks (Fig. 3G); *Snail* mRNA levels were enhanced 3 fold (Fig. S5). PS reversed the induction of Snail protein by TGFβ1 in HMLER cells, but had no significant effect on *Snail* mRNA levels (Fig. S5). Snail protein is highly unstable and its degradation is tightly regulated by canonical Wnt signaling and GSK-3β [36, 38]. As shown in Fig. 3B, PS enhanced GSK-3β kinase activity (decreased

phosphorylation on serine 9) in HMLER cells. In addition, the proteasome inhibitor MG-132 and lithium chloride, a potent GSK-3β inhibitor [39], abolished PS's inhibition of Snail (Fig. 3F). These results suggest that PS suppresses Snail levels by enhancing GSK-3β activity to promote its ubiquitination and degradation. More importantly, PS blocked the induction of EMT by TGFβ1 and abolished the generation of $CD44^{high}/CD24^{low}$ cells (Fig. 3G), and this result was also confirmed by detecting the expression levels of E-cadherin and vimentin (Fig. S3B). As Wnt signaling, alone or in combination with TGFβ-Snail signaling, can lead to EMT, and inhibition of these signaling can block EMT and lead to reversal of the mesenchymal phenotype [40, 41], it appears that the suppressive effects of PS on Wnt/β-catenin signaling and Snail expression contribute to its ability to block EMT.

PS inhibits the tumorigenicity of CSCs in immunodeficient mice

We tested whether PS inhibits breast CSCs *in vivo*. Immunodeficient mice were started on 100 mg/kg PS or vehicle by oral gavage one week prior to subcutaneous implantation to each flank of 2,000 SK-3rd cells and continued for another 45 days (prevention protocol). As shown in Fig. 4A (top panel), 6 out of 7 animals in the control group developed tumors, while only 3 animals in the PS-treated group developed tumors after 45 days (p=0.06). This finding suggests that PS can impair the *in vivo* tumor-initiating ability of CSCs. We then investigated the ability of PS to inhibit the growth of already established tumors initiated by breast CSCs (treatment protocol). $HMLER^{TGF\beta1}$ cells were implanted into the most cephalad mammary gland of immunodeficient mice. We started administering PS 150 mg/kg/d or vehicle (corn oil) orally when tumors reached a volume of ~50 mm^3. PS had a marked inhibitory effect on the growth of these xenografts, generating tumor stasis, with its effect becoming statistically significant after the third week. At sacrifice (week 6), the tumor volume of the control group was 490±135 mm^3 (*mean ± SEM*), while of the PS-treated group it was 125 ± 34 mm^3, representing growth inhibition of 83.0% by PS (Fig. 4A, lower panel).

As PS suppresses the protein level of β-catenin and inhibits its cytoplasmic/nuclear localization *in vitro*, we determined the level of β-catenin in HMLER xenografts. In xenografts from the vehicle group, β-catenin signaling remained activated in many HMLER cells, since β-catenin mainly localized in the cytoplasm and nuclei. However, in PS-treated xenografts, most β-catenin localized in the cell membrane (Fig. 4D, top panel). By determining protein levels in HMLER xenografts with immunoblot, we found that tumors in the treatment group expressed lower levels of β-catenin than controls (Fig. 4C). These findings are consistent with our *in vitro* results with HMLER cells and MDAMB-231 cells (Fig. 3B, 3C, 3D, S4A and S4B). We also stained HMLER xenografts by immunohistochemistry for the EMT marker vimentin. There was high intensity staining of vimentin in vehicle-treated samples. In contrast, PS-treated xenografts exhibited much less vimentin staining (50.8% lower than control group), indicating that PS increased epithelial differentiation relative to vehicle (Fig. 4D, middle panel). Similar results were observed in MDAMB-231 xenografts (Fig. S6). GSK-3β phosphorylation on serine 9 was elevated in PS treated HMLER xenografts, explaining the lower levels of Snail and β-catenin (Fig. 4C). These *in vivo* results are in agreement with our observation that PS blocked TGFβ1-induced EMT *in vitro* (Fig. 3G). PS also reduced the expression of CD44, a downstream target of β-catenin signaling, in HMLER xenografts (Fig. 4C). Combined with the findings that HMLER xenografts treated with PS had fewer $CD44^{high}/CD24^{low}$ tumor cells (Fig. 4B), these data strongly support the notion that PS specifically targets breast CSCs *in vivo*. To obtain further support, we tested the *in vivo* effect of PS on CSCs using ALDH1, another widely used marker for both normal and malignant human breast stem cells [3, 42]. As shown in Fig. 4D (lower panel), ALDH1 positive staining was greatly reduced in PS-treated xenografts compared with vehicle-treated samples.

Discussion

Our findings indicate that the novel compound PS effectively inhibits breast CSCs both *in vitro* and in animal cancer models. Since CSCs are required for both tumor initiation and development, we reason that their selective targeting by PS accounts for most, if not all, of PS's inhibitory effect on tumor growth.

In this study, we evaluated the effect of PS on CSCs using two breast cell lines generated by genetic modification or drug selection; both were resistant to conventional cancer drugs. Our data demonstrate that PS kills CSCs as effectively as non-CSCs, including in this case the parental cells of the two CSC cell lines. A remarkable feature of this effect was that prolonged treatment with PS (12 days) killed CSCs more effectively and selectively than short-term term treatment (48 h). Whether this finding will be relevant to the envisioned anticancer application of PS remains to be seen. Another striking finding was that the ability of PS to inhibit CSCs appears not to rely on its cytotoxicity; even at low (non-cytotoxic) concentrations, PS impaired quite effectively CSCs' ability of mammosphere formation, which is an important indicator of the self-renewal property of CSCs [27].

In agreement with its *in vitro* effects, PS suppressed tumor initiation *in vivo*. Administered orally, PS reduced tumor incidence by half in a cancer prevention animal model that employed xenografts of the highly tumorigenic SK-3rd cells in immunocompromised mice. The therapeutic effect of PS (administration to animals with already formed orthotopic breast cancer tumors), was even more pronounced: tumor growth was inhibited by 83.0% after 42 days of its oral administration. Attesting to its effect on CSCs, PS reduced significantly the proportion of CD44^{high}/CD24^{low} cells in the tumor cell population. This finding should be viewed in the light of recent clinical studies showing that in breast tumors conventional chemotherapy enriches CD44^{high}/CD24^{low} tumor cells. The latter effect, being in contrast to the action of PS, is considered responsible for chemoresistance and tumor relapse [5, 25].

The effect of PS on CSCs is mediated through an elaborate effect on cell signaling. *In vitro*, PS had a pronounced effect on the Wnt signaling cascade, reducing the levels of β-catenin in the nucleus where it exerts its transcriptional activity [43]. The functional significance of the reduced nuclear levels of β-catenin is underscored by the 4-fold suppressed β-catenin transcriptional activity in response to PS monitored by the luciferase assay (Fig. 3A). The low levels of β-catenin are due, at least in part, to reduced phosphorylation of GSK-3β, which in turn enhances its kinase activity, resulting in β-catenin degradation. The relocalization of β-catenin, which is controlled by a complex set of mechanisms, is also critical for the suppressive effect of PS on Wnt/β-catenin signaling [44–48]. APC, which forms the degradation complex with GSK3β, is involved in the cytoplasmic-nuclear shuttling of β-catenin by forming an APC/β-catenin complex [45]. Considering the fact that sulindac could increase APC expression both *in vitro* and *in vivo* [49–51], and that PS suppresses phosphorylation of GSK-3β, it is intriguing to explore the role of APC/GSK-3β in PS-induced relocalization of β-catenin. The effect of PS on Wnt signaling is not restricted to cultured cells. Indeed, a similar effect on β-catenin signaling by PS was noted *in vivo*. PS treatment of mice bearing HMLER xenografts strongly reduced β-catenin levels (75.1% by immunoblotting) in these xenografts, with most of the remaining β-catenin re-localized to the cell membrane. Our data are consistent with recent findings on the essential role of Wnt signaling in maintaining the stem cell state and tumorigenicity of HMLER cells [8]. Current understanding of deregulated Wnt/β-catenin signaling in tumor initiation and progression highlights the potential of blocking this pathway for cancer treatment; several experimental agents are being evaluated as Wnt signaling inhibitors [12, 52]. However, it appears that prolonged use of such agents might cause side effects including those for the skin and

intestine where β-catenin signaling is crucial for tissue renewal [53]. Considering our previous work showing that PS is very safe in various preclinical models [22, 23], our findings reinforce the notion that PS might be useful in breast cancer chemoprevention and chemotherapy.

The induction in HMLEs of EMT results in the expression of stem cell markers and formation of mammospheres [6]. At concentrations around its IC^{50} for growth inhibition, PS suppressed nearly completely the EMT of HMLER cell that was initiated by TGFβ1 (57.2% to 1.4-0.5%). In addition to the flow cytometry data monitoring the expression of CD24 and CD44, PS changed in the appropriate direction the expression of epithelial (E-cadherin) and mesenchymal (Snail and vimentin) markers. This effect was also documented *in vivo* (suppressed vimentin expression in xenografts). Given the role of Wnt signaling in EMT [8, 36, 54] and the effect of PS on both, it is conceivable that the two effects are linked. Furthermore, based on the emerging impact of EMT on tumor cell migration and invasion, we speculate that PS could inhibit tumor metastasis.

In conclusion, our data establish a very strong chemotherapeutic effect of PS in a preclinical model of breast cancer that is accompanied by significant suppression of CSCs and inhibition of EMT. Inhibition of Wnt/β-catenin signaling by PS appears to be a critical mediator of these effects. Given these effects and evidence for its safety, PS merits further evaluation as a promising agent against breast cancer.

Supplementary Material

Refer to Web version on PubMed Central for supplementary material.

Acknowledgments

This work was supported by grants from the National Institutes of Health National Cancer Institute (R01CA139454) and the Department of Defense (W81XWH1010873).

References

1. Molyneux G, et al. BRCA1 basal-like breast cancers originate from luminal epithelial progenitors and not from basal stem cells. Cell Stem Cell. 2010; 7(3):403–417. [PubMed: 20804975]
2. Zhou BB, et al. Tumour-initiating cells: challenges and opportunities for anticancer drug discovery. Nat Rev Drug Discov. 2009; 8(10):806–823. [PubMed: 19794444]
3. Ginestier C, et al. ALDH1 is a marker of normal and malignant human mammary stem cells and a predictor of poor clinical outcome. Cell Stem Cell. 2007; 1(5):555–567. [PubMed: 18371393]
4. Charafe-Jauffret E, et al. Breast cancer cell lines contain functional cancer stem cells with metastatic capacity and a distinct molecular signature. Cancer Res. 2009; 69(4):1302–1313. [PubMed: 19190339]
5. Al-Hajj M, et al. Prospective identification of tumorigenic breast cancer cells. Proc Natl Acad Sci U S A. 2003; 100(7):3983–3988. [PubMed: 12629218]
6. Mani SA, et al. The epithelial-mesenchymal transition generates cells with properties of stem cells. Cell. 2008; 133(4):704–715. [PubMed: 18485877]
7. Gupta PB, et al. Identification of selective inhibitors of cancer stem cells by high-throughput screening. Cell. 2009; 138(4):645–659. [PubMed: 19682730]
8. Scheel C, et al. Paracrine and autocrine signals induce and maintain mesenchymal and stem cell States in the breast. Cell. 2011; 145(6):926–940. [PubMed: 21663795]
9. Santisteban M, et al. Immune-induced epithelial to mesenchymal transition in vivo generates breast cancer stem cells. Cancer Res. 2009; 69(7):2887–2895. [PubMed: 19276366]
10. Rich JN, et al. Cancer stem cells in radiation resistance. Cancer Res. 2007; 67(19):8980–8984. [PubMed: 17908997]

11. Al-Ejeh F, et al. Breast cancer stem cells: treatment resistance and therapeutic opportunities. Carcinogenesis. 2011; 32(5):650–658. [PubMed: 21310941]
12. Takebe N, et al. Targeting cancer stem cells by inhibiting Wnt, Notch, and Hedgehog pathways. Nat Rev Clin Oncol. 2011; 8(2):97–106. [PubMed: 21151206]
13. Barker N, Clevers H. Mining the Wnt pathway for cancer therapeutics. Nat Rev Drug Discov. 2006; 5(12):997–1014. [PubMed: 17139285]
14. Ulrich CM, Bigler J, Potter JD. Non-steroidal anti-inflammatory drugs for cancer prevention: promise, perils and pharmacogenetics. Nat Rev Cancer. 2006; 6(2):130–140. [PubMed: 16491072]
15. Hanif R, et al. Effects of nonsteroidal anti-inflammatory drugs on proliferation and on induction of apoptosis in colon cancer cells by a prostaglandin-independent pathway. Biochem Pharmacol. 1996; 52(2):237–245. [PubMed: 8694848]
16. Shiff B, Rigas SJ. The role of cyclooxygenase inhibition in the antineoplastic effects of nonsteroidal antiinflammatory drugs (NSAIDs). J Exp Med. 1999; 190(4):445–450. [PubMed: 10449515]
17. Qiu W, et al. Chemoprevention by nonsteroidal anti-inflammatory drugs eliminates oncogenic intestinal stem cells via SMAC-dependent apoptosis. Proc Natl Acad Sci U S A. 2010; 107(46): 20027–20032. [PubMed: 21041628]
18. Tinsley HN, et al. Inhibition of PDE5 by sulindac sulfide selectively induces apoptosis and attenuates oncogenic Wnt/beta-catenin mediated transcription in human breast tumor cells. Cancer Prev Res (Phila). 2011
19. Seo AM, et al. Sulindac induces apoptotic cell death in susceptible human breast cancer cells through, at least in part, inhibition of IKKbeta. Apoptosis. 2009; 14(7):913–922. [PubMed: 19526344]
20. Knights KM, Tsoutsikos P, Miners JO. Novel mechanisms of nonsteroidal anti-inflammatory drug-induced renal toxicity. Expert Opin Drug Metab Toxicol. 2005; 1(3):399–408. [PubMed: 16863452]
21. Lazzaroni GB, Porro M. Management of NSAID-induced gastrointestinal toxicity: focus on proton pump inhibitors. Drugs. 2009; 69(1):51–69. [PubMed: 19192936]
22. Mackenzie GG, et al. Phospho-sulindac (OXT-328), a novel sulindac derivative, is safe and effective in colon cancer prevention in mice. Gastroenterology. 2010; 139(4):1320–1332. [PubMed: 20600034]
23. Huang L, et al. The novel phospho-non-steroidal anti-inflammatory drugs, OXT-328, MDC-22 and MDC-917, inhibit adjuvant-induced arthritis in rats. Br J Pharmacol. 2011; 162(7):1521–1533. [PubMed: 21175575]
24. Elenbaas B, et al. Human breast cancer cells generated by oncogenic transformation of primary mammary epithelial cells. Genes Dev. 2001; 15(1):50–65. [PubMed: 11156605]
25. Yu F, et al. let-7 regulates self renewal and tumorigenicity of breast cancer cells. Cell. 2007; 131(6):1109–1123. [PubMed: 18083101]
26. Eyler JN, Rich CE. Survival of the fittest: cancer stem cells in therapeutic resistance and angiogenesis. J Clin Oncol. 2008; 26(17):2839–2845. [PubMed: 18539962]
27. Pastrana E, Silva-Vargas V, Doetsch F. Eyes wide open: a critical review of sphere-formation as an assay for stem cells. Cell Stem Cell. 2011; 8(5):486–498. [PubMed: 21549325]
28. Vermeulen L, et al. Wnt activity defines colon cancer stem cells and is regulated by the microenvironment. Nat Cell Biol. 2010; 12(5):468–476. [PubMed: 20418870]
29. Yamashita T, et al. Activation of hepatic stem cell marker EpCAM by Wnt-beta-catenin signaling in hepatocellular carcinoma. Cancer Res. 2007; 67(22):10831–10839. [PubMed: 18006828]
30. Malanchi I, et al. Cutaneous cancer stem cell maintenance is dependent on beta-catenin signalling. Nature. 2008; 452(7187):650–653. [PubMed: 18385740]
31. Yang W, et al. Wnt/beta-catenin signaling contributes to activation of normal and tumorigenic liver progenitor cells. Cancer Res. 2008; 68(11):4287–4295. [PubMed: 18519688]
32. Brown WA, et al. Inhibition of beta-catenin translocation in rodent colorectal tumors: a novel explanation for the protective effect of nonsteroidal antiinflammatory drugs in colorectal cancer. Dig Dis Sci. 2001; 46(11):2314–2321. [PubMed: 11713928]

33. Rice PL, et al. Sulindac metabolites induce caspase- and proteasome-dependent degradation of beta-catenin protein in human colon cancer cells. Mol Cancer Ther. 2003; 2(9):885–892. [PubMed: 14555707]
34. Boon EM, et al. Sulindac targets nuclear beta-catenin accumulation and Wnt signalling in adenomas of patients with familial adenomatous polyposis and in human colorectal cancer cell lines. Br J Cancer. 2004; 90(1):224–229. [PubMed: 14710233]
35. Mosimann C, Hausmann G, Basler K. Beta-catenin hits chromatin: regulation of Wnt target gene activation. Nat Rev Mol Cell Biol. 2009; 10(4):276–286. [PubMed: 19305417]
36. Yook JI, et al. A Wnt-Axin2-GSK3beta cascade regulates Snail1 activity in breast cancer cells. Nat Cell Biol. 2006; 8(12):1398–1406. [PubMed: 17072303]
37. Yang J, Weinberg RA. Epithelial-mesenchymal transition: at the crossroads of development and tumor metastasis. Dev Cell. 2008; 14(6):818–829. [PubMed: 18539112]
38. Zhou BP, et al. Dual regulation of Snail by GSK-3beta-mediated phosphorylation in control of epithelial-mesenchymal transition. Nat Cell Biol. 2004; 6(10):931–940. [PubMed: 15448698]
39. Stambolic V, Ruel L, Woodgett JR. Lithium inhibits glycogen synthase kinase-3 activity and mimics wingless signalling in intact cells. Curr Biol. 1996; 6(12):1664–1668. [PubMed: 8994831]
40. Medici D, Hay ED, Goodenough DA. Cooperation between snail and LEF-1 transcription factors is essential for TGF-beta1-induced epithelial-mesenchymal transition. Mol Biol Cell. 2006; 17(4): 1871–1879. [PubMed: 16467384]
41. Medici D, Hay ED, Olsen BR. Snail and Slug promote epithelial-mesenchymal transition through beta-catenin-T-cell factor-4-dependent expression of transforming growth factor-beta3. Mol Biol Cell. 2008; 19(11):4875–4887. [PubMed: 18799618]
42. Huang EH, et al. Aldehyde dehydrogenase 1 is a marker for normal and malignant human colonic stem cells (SC) and tracks SC overpopulation during colon tumorigenesis. Cancer Res. 2009; 69(8):3382–3389. [PubMed: 19336570]
43. Klaus W, Birchmeier A. Wnt signalling and its impact on development and cancer. Nat Rev Cancer. 2008; 8(5):387–398. [PubMed: 18432252]
44. Ryo A, et al. Pin1 regulates turnover and subcellular localization of beta-catenin by inhibiting its interaction with APC. Nat Cell Biol. 2001; 3(9):793–801. [PubMed: 11533658]
45. Henderson BR. Nuclear-cytoplasmic shuttling of APC regulates beta-catenin subcellular localization and turnover. Nat Cell Biol. 2000; 2(9):653–660. [PubMed: 10980707]
46. Zhang N, et al. FoxM1 promotes beta-catenin nuclear localization and controls Wnt target-gene expression and glioma tumorigenesis. Cancer Cell. 2011; 20(4):427–442. [PubMed: 22014570]
47. Du C, et al. Protein kinase D1-mediated phosphorylation and subcellular localization of beta-catenin. Cancer Res. 2009; 69(3):1117–1124. [PubMed: 19141652]
48. Wu X, et al. Rac1 activation controls nuclear localization of beta-catenin during canonical Wnt signaling. Cell. 2008; 133(2):340–353. [PubMed: 18423204]
49. Schnitzler M, Dwight T, Robinson BG. Sulindac increases the expression of APC mRNA in malignant colonic epithelial cells: an in vitro study. Gut. 1996; 38(5):707–713. [PubMed: 8707116]
50. Kishimoto Y, et al. Sulindac and a cyclooxygenase-2 inhibitor, etodolac, increase APC mRNA in the colon of rats treated with azoxymethane. Gut. 2000; 47(6):812–819. [PubMed: 11076880]
51. Kishimoto Y, et al. Effects of long-term administration of sulindac on APC mRNA and apoptosis in colons of rats treated with azoxymethane. J Cancer Res Clin Oncol. 2002; 128(11):589–595. [PubMed: 12458338]
52. Curtin MV, Lorenzi JC. Drug discovery approaches to target Wnt signaling in cancer stem cells. Oncotarget. 2010; 1(7):563–577. [PubMed: 21317452]
53. Reya T, Clevers H. Wnt signalling in stem cells and cancer. Nature. 2005; 434(7035):843–850. [PubMed: 15829953]
54. Yook JI, et al. Wnt-dependent regulation of the E-cadherin repressor snail. J Biol Chem. 2005; 280(12):11740–11748. [PubMed: 15647282]

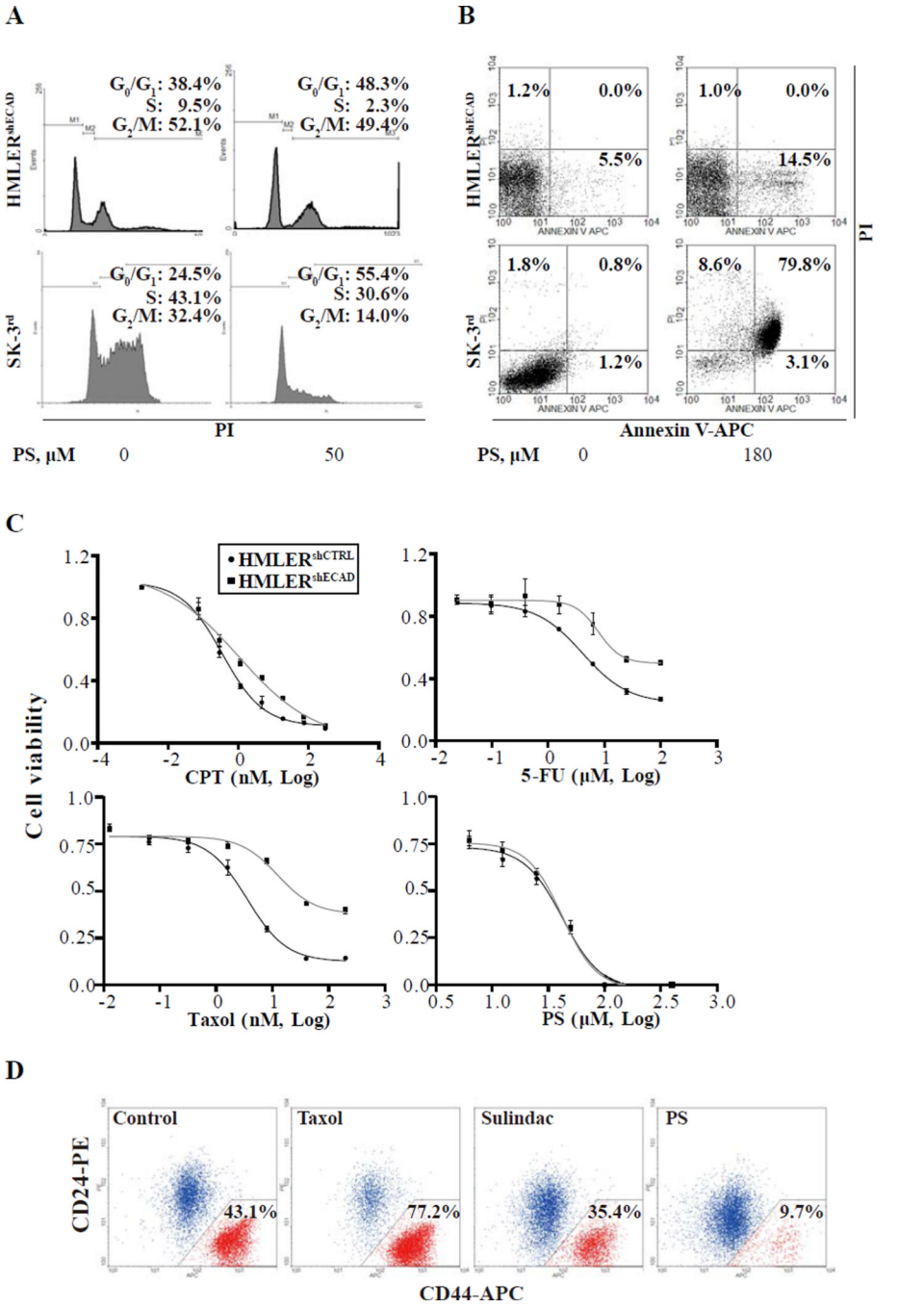

Fig. 1. PS effectively and selectively eliminates breast CSCs *in vitro*

(**A**) The indicated cell lines were treated with 50 μM PS for 24 h, stained with propidium iodide and analyzed by flow cytometry for cell cycle phase distribution as in *Methods*. The experiment was repeated 3 times and representative results are shown. PS significantly reduced the percentage of cells in S phase in HMLER^{shECAD} and SK-3rd ($P < 0.05$ compared with DMSO control). The percentage of cells in each phase is shown. (**B**) Cells were treated with 180 μM PS for 24 h, stained with propidium iodide and Annexin V-APC and analyzed by flow cytometry, as in Methods. Annexin V(+)/PI(-) = apoptosis; Annexin V(+)/PI(+) = end-stage apoptosis (secondary necrosis). The experiment was repeated 3 times

and representative results are shown. PS significantly increased the percentage of dead HMLER^{shECAD} and SK-3rd cells ($P < 0.01$ compared with DMSO control). (**C**) Inhibition curves and IC^{50}s of each compound for the indicated cell lines treated with PS for 48 h Cell viability was determined by MTT assay as in Methods. (**D**) Sorted HMLER CD44^{high}/CD24^{low} and CD44^{low}/CD24^{high} cells were mixed at a ratio about 1:1 and plated in 6-well plates. After incubation with DMSO, PS (30 μM), Taxol (10 nM) or sulindac (700 μM) respectively for 7 days as in Methods, cells were stained for CD24/CD44 and analyzed by flow cytometry.

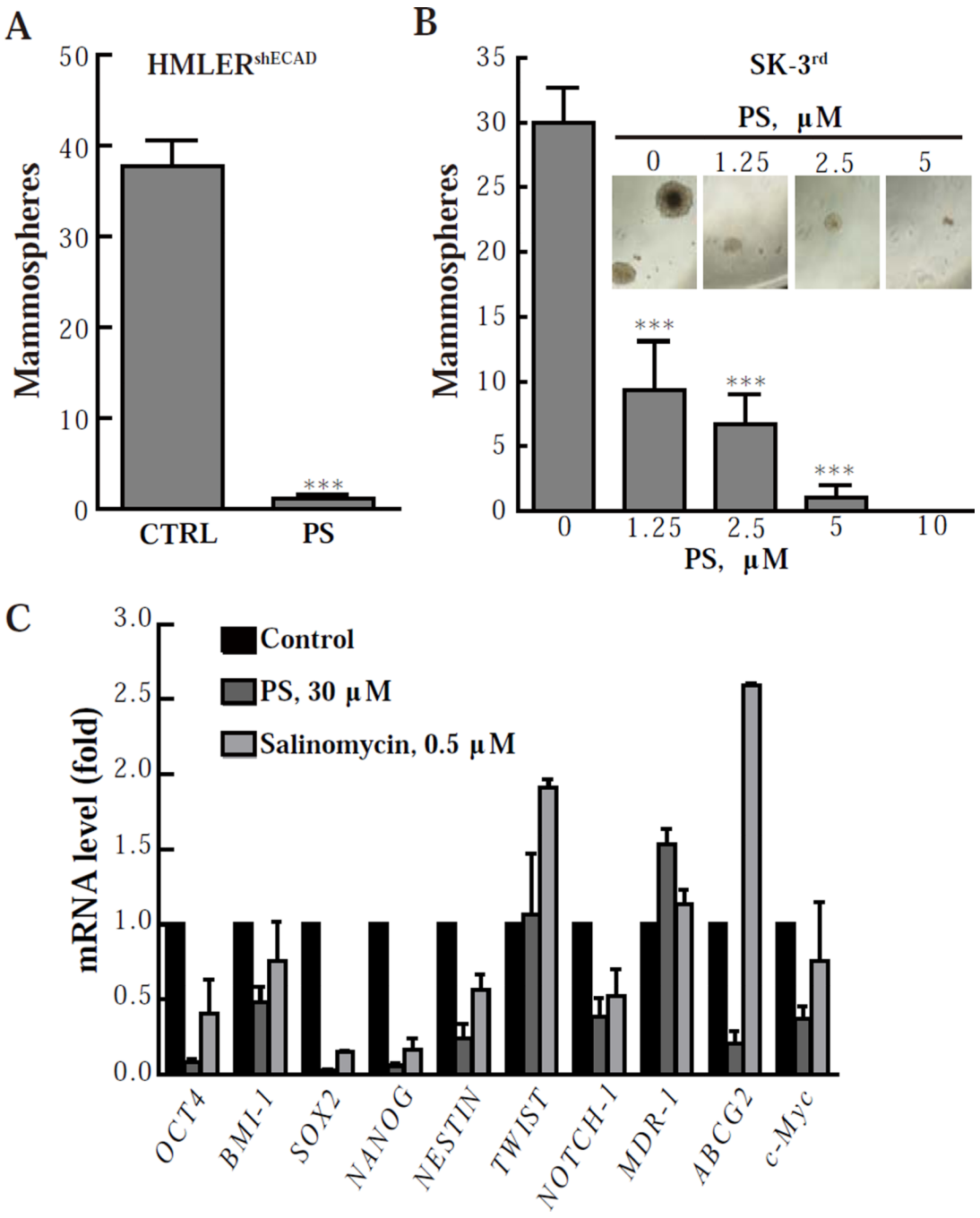

Fig. 2. PS impairs the mammosphere-formation ability of breast CSCs

(**A & B**) HMLER^{shECAD} cells were treated with 30 μM PS for 48 h, and after removing the remaining compound were cultured for 14 days in serum-free culture media as floating cells to form mammospheres. SK-3rd cells were cultured with various concentrations of PS for 12 days to form mammospheres. 300 HMLER^{shECAD} or SK-3rd cells were seeded in each well of 96 well plates. ***, $P < 0.001$ compared with control. (**C**) HMLER^{shECAD} cells were treated with PS or salinomycin for 24 h and the relative mRNA levels of the indicated genes were determined by real-time PCR. *, $P < 0.05$; **, $P < 0.01$; ***, $P < 0.001$ compared to control.

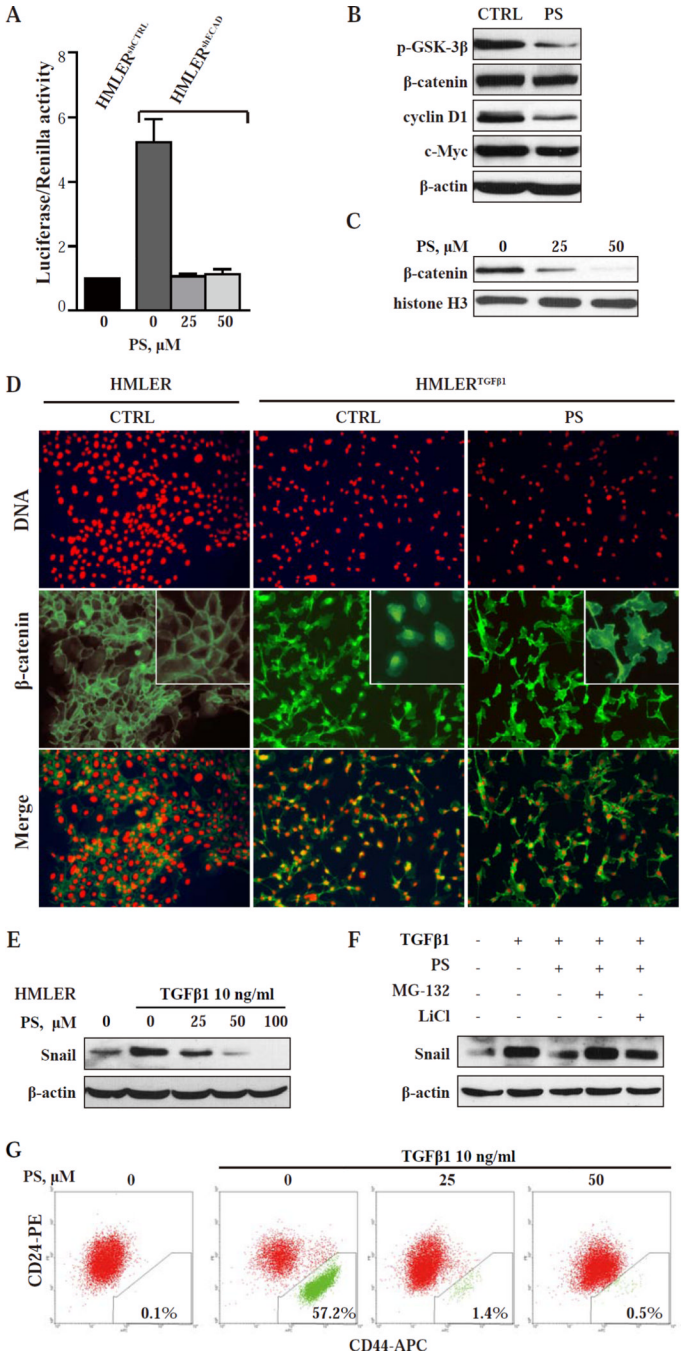

Fig.3. PS targets the Wnt/β-catenin pathway and reduces Snail expression blocking EMT and preventing the generation of CSCs

(**A**) TCF/LEF transcriptional activity was tested by TOPFlash (TCF-LEF reporter) and FOPFlash (mutated binding sites). β-catenin/TCF-LEF activity is shown as TOP over FOP firefly luciferase activity, normalized to internal control Renilla luciferase activity. ***, $P < 0.001$ compared with control. (**B**) Immunoblot of the indicated proteins in HMLER^{shECAD} cells after 36-h treatment with 30 μM PS. Loading control: β-actin. (**C**) Nuclear β- catenin levels in HMLER^{shECAD} cells treated with PS determined by immunoblotting. Loading control: histone H3. (**D**) Immunofluorescence images of HMLER and HMLER^{TGFβ1} cells treated as shown for 24 h. *Upper row*: staining with PI visualizes the nuclei. *Middle row*:

Staining with an 23 anti-β-catenin mAb. In HMLER cells, β-catenin is mainly in the cell membrane. In vehicle treated HMLER$^{TGF\beta1}$ cells, β-catenin is mainly nuclear/cytoplasmic, shifting predominantly to the cell membrane after PS treatment. *Lower row*: The merged images of the two rows above. Magnification: 20x. (**E**) HMLER cells were treated for 24 h with various concentrations of PS and with or without TGFβ1, the EMT-inducing agent. Protein levels of Snail were determined by immunoblotting. Loading control: β-actin. (**F**) HMLER cells were treated with the indicated compounds for 8 h. MG-132 or LiCl was added 10 min before other treatments started, as in Methods. (**G**) HMLER cells were incubated with TGFβ1 and the ind icated concentrations of PS for 14 days. CD24/CD44 expression profiles were then analyzed by flow cytometry as in Methods.

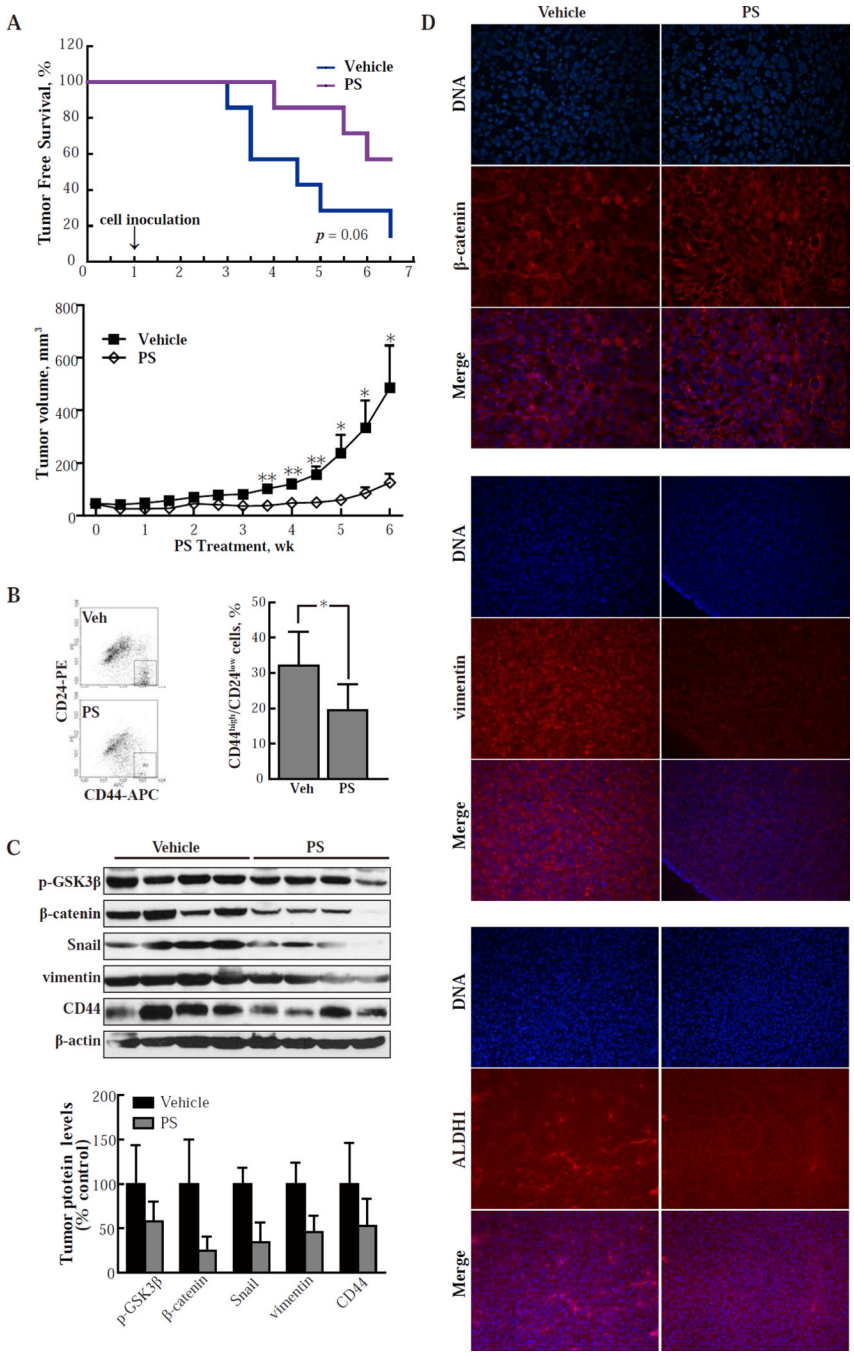

Fig. 4. PS inhibits the tumorigenicity of CSCs in nude mice

(**A**) *Upper panel*: SK-3rd cells (2,000 per animal) were inoculated into immunodeficient mice. Treatment with vehicle or PS 100 mg/kg po daily 5x/wk started 1 wk prior to inoculation (prevention protocol). PS increased tumor-free survival by 50% (p=0.06; n=7/group). *Lower panel*: immunodeficient mice were inoculated with HMLER$^{TGF\beta1}$ cells (50,000/mouse) and treatment with vehicle or PS 150 mg/kg po daily 5x/wk started when the tumor reached the indicated size (treatment protocol). Values are mean±SEM; n=10/group. *, $P < 0.05$; **, $P < 0.01$ compared to control. (**B**) Single cell suspensions from HMLER$^{TGF\beta1}$ xenografts obtained by collagenase treatment as in Methods were stained for

CD24/CD44 and analyzed by flow cytometry. In each group, 4 xenografts were studied and representative results are shown on the left. *, $P < 0.05$. (**C**) Protein levels in HMLER$^{TGF\beta1}$ xenografts were determined by immunoblotting and their band intensity (normalized to β-actin) is depicted in the graph. Values are mean±SD. *, $P < 0.05$; **, $P < 0.01$ compared to control. (**D**) Immunofluorescence images of tissue sections from HMLER$^{TGF\beta1}$ xenografts from the study depicted in A, lower panel (treatment protocol). *Upper panel*: staining with DAPI visualizes the nuclei and staining with an anti-β-catenin mAb reveals its distribution in the cells. The merged images of the two rows above are also shown. Analogous images from tissue sections stained for vimentin *(middle panel*) and ALDH1 (*lower panel*). Treatment with PS caused β-catenin to relocalize to the cell membrane. It also suppressed the expression of both vimentin and ALDH1, indicating suppression of EMT and near elimination of CSCs, respectively. Magnification: 20x.

Table 1

The growth inhibitory effect of conventional cancer drugs and PS

	IC_{50}			IC_{50}		
Compounds	**HMLER^{shCTRL}**	**HMLER^{shECAD}**	**Drug resistance (fold)**	**SKBR3**	**SK-3rd**	**Drug resistance (fold)**
Camptothecin (nM)	0.78	3.6	4.7	0.78	13.6	17.4
Taxol(nM)	4.8	53.2	11.1	0.12	≫2	≫16.7
Fluorouracil(μM)	6.2	60.8	9.9	N/A	N/A	N/A
PS(μM)	31.1	33.2	1.1	62.1	57.4	0.9

N/A, not available.

Abbreviations: CPT, camptothecin: 5-FU, fluorouracil: HMLER, *Ras*-transformed HMLE: PS, phophosulindac.